



INŽENÝRSKÁ MECHANIKA 2005

NÁRODNÍ KONFERENCE

s mezinárodní účastí

Svratka, Česká republika, 9. - 12. května 2005

INFLUENCE OF SURFACE ROUGHNESS ON SPRAY COOLING INTENSITY IN HIGH TEMPERATURE APPLICATIONS

A. Horák^{*}, P. Střítecký^{**}

Summary: *The paper deals with determination of surface roughness influence on spray cooling intensity. The questions of the surface quality on the heat transfer and the Leidenfrost temperature in this area have not yet been properly answered. Previous investigations showed that such an influence may exist. The main aim of this study is therefore to verify this hypothesis by using statistical methods and to construct exact mathematical model describing given problem. The cooling experimental stand using a steel testing plate was developed and high temperature experiments (up to 1200°C) with various surface roughness parameters were accomplished. The paper presents measured experiments, data evaluation and processes and the influence of surface manufacturing methods, e.g. rolled, burnished, fine and rough grind surface, on cooling process.*

1 Introduction

The influence of surface quality on heat transfer in high temperature applications has been widely studied. Up to the present there has not been accepted a general theory relating to heat transfer with surface roughness of metallic materials. Previous studies have shown different approaches and techniques. The paper considered the experimental investigations of spray quenching described for different surfaces (aluminium plates, stainless steels ...) by Bernardin J.D. & Mudawar I.; Raudenský M., Horský J. & Kotrbáček P., and a single droplet effect for cooling and Leidenfrost temperature as well. Additionally, the oxide scale influences on heat transfer in continuous casting, published in the article (Köhler Ch. & Collective 1990) were examined.

In this paper, the influences of different manufacturing methods on heat transfer and the Leidenfrost temperature are presented. Previous experiments were done for the application of continuous casting indicating such functionality. Fig.1 shows a typical temperature-time history of sprayed steel. The curve can be divided into four distinct areas, with different heat transfer characteristics. The cooling of steel begins in the range of Film Boiling Regime, where the quenching process starts rather slowly as a liquid-solid contact and is prevented by a formation of isolating vapour layer. The temperature moment, where this vapour film collapses, is designated as Leidenfrost Point, below this point Transition Boiling Regime

^{*} Ing. Aleš Horák: Heat Transfer and Fluid Flow Laboratory, Faculty of Mechanical Engineering, Brno University of Technology; Technická 2; 616 69 Brno; tel.: +420.541.143.281; e-mail: horak@lu.fme.vutbr.cz

^{**} Ing. Pavel Střítecký: Department of Control and Instrumentation, Faculty of Electrical Engineering and Communication, Brno University of Technology; Kolejní 4; 616 69 Brno; tel.: +420.541.143.641; e-mail: xstrit02@stud.feec.vutbr.cz

occurs. During this regime water droplets partly moisten the steel surface of the metal and this partial liquid-solid contact increases cooling rate. **Nucleate Boiling Regime** is the most intensive phase of heat transfer where bubbles are formed. **Single-Phase Regime** is the area where vapour is formed and heat transfer is caused only by convection.

As the vapour layer is thin (in order of μm) surface roughness profile must be considered. Cavities and jags could cause a protection against vapour layer forming as well as these surface dislocations can increase the bubble nucleation resulting in the heat flux increase.

A typical metallic surface is made up of many such imperfections, including pits, scratches and bumps. For more detailed recognition, all usual roughness parameters were measured by mechanical and optical methods and also photos recorded by electron microscope were taken. To illustrate the situation, Fig.2 shows the distribution of heat transfer coefficient (HTC) for original rolled, burnished, fine and rough grind surfaces, used for experiments.

It must be also mentioned that thermal stress (especially in high-temperature areas) causes the degradation of metallic surfaces. In this study, the statistical methods and tests were used to explore the effects of surface roughness on heat transfer.

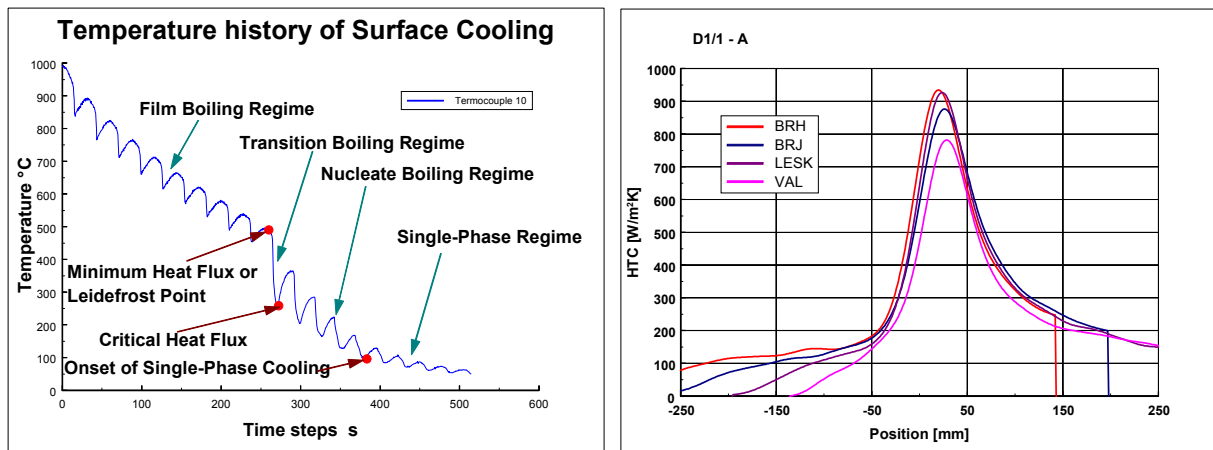


Fig. 1: (left) *Temperature history of Surface Cooling*

Fig. 2: (right) *HTC distribution in the area for original rolled, burnished, fine and rough grind surfaces. Position 0 is nozzle axis*

2 Testing Equipment

The laboratory stand developed for testing the nozzles usually used for continuous casting was built, see Photo 1. A steel frame holds three major parts of the stand: stainless steel test plate, driving mechanism with a nozzle and heater. The experimental stand allows recording the current temperature of the sprayed test plate and the actual position in time of a moving nozzle.

The test plate is made of austenitic steel to prevent the surface from oxidation and decrease the degradation of material due to thermal stresses. There are holes drilled into the plate where the thermocouples are placed. The shielded thermocouples of type K and a diameter of 1.5 mm are used for temperature monitoring. The sample is insulated from surroundings in the frame body to provide heat transfer only by sprayed water. For this study, two different plate types were prepared. The first group of experiments with the mist nozzle

type was measured on sample 1. The spray height for this nozzle was 300mm. The second group of experiments was done for the flat jet nozzles and the full cone nozzles (photo 2) on sample 2. The spray height for the second group was 125 mm. The shape of the plate, surface manufacturing and the distribution of thermocouples used for these tests can be seen in Fig. 3 and Photo 3. Total 18 thermocouples in three rows and six columns were used. The spraying nozzle first reaches the first column (thermocouples 1, 7 and 13), then the second column (thermocouples 2, 8, 14) etc. The axis of the tested nozzle is aimed to the central row of thermocouples.

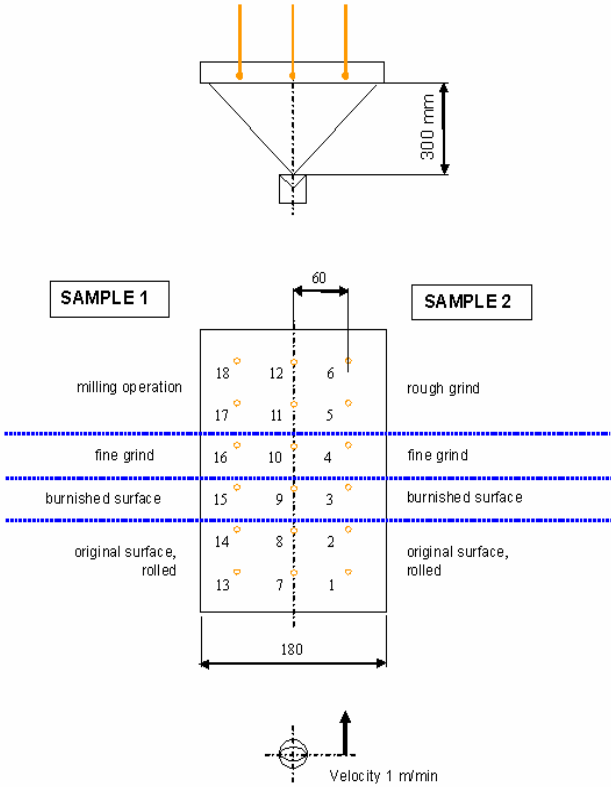


Photo 1 (left) Laboratory testing bench

Fig. 3 (right) Testing plate scheme with thermocouples positions and surface manufacturing methods



Photo 2 Water nozzles used in tests

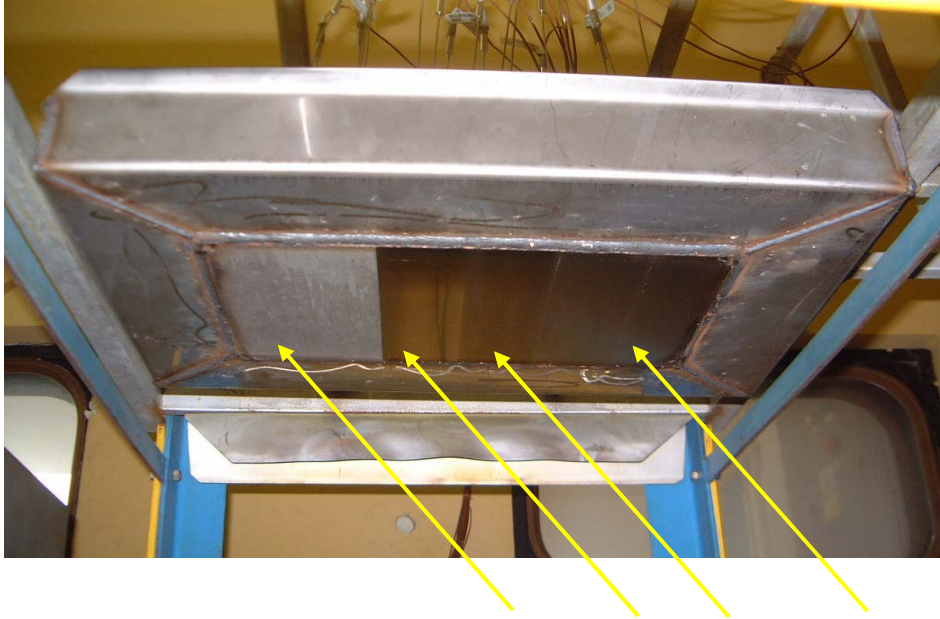


Photo 3: Test plate, surface quality: left side rolled, burnished, fine grind, rough grind

The driving mechanism moving the nozzle under the plate is described in Fig.4. The rotation of a step motor and consequently the speed of nozzle motion are controlled by a computer. The speed of motion was set to 1.0 m/min when spraying, i.e. during the movement from the negative to positive values of the position running with open deflector. On the way back to the initial position, the deflector is closed and the speed is doubled to 2.0 m/min to reduce the time without spraying. The deflector is pneumatically driven and controlled by the computer. The experimental program uses distilled water. This is very unusual for the experiments with spray cooling. The reason was not to contaminate the sprayed surface by salts from the evaporated water.

The third major part of the test bench is an **electric furnace** used for heating of the plate to the initial temperature. The furnace moves on rails. It is placed under the test plate when the experiment is prepared and the gap between the furnace edges and the plate is filled with insulation. The plate is heated at the beginning of the experiment up to an initial temperature. A temperature of 1000° C was set as the initial. The test plate is placed into a jig. It allows moving the plate up, removing the furnace back and positioning the nozzle with the driving mechanism to the space under the plate.

The computer with the data acquisition system Keithley is located outside the spray box in a control room. It monitors the process of heating, controls the experiment and records the data from thermocouples and opto-electronic sensors.

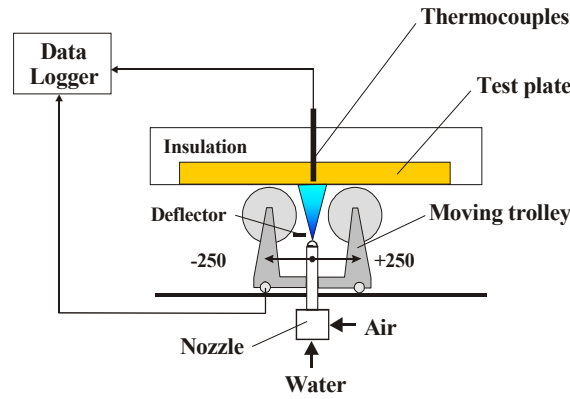


Fig. 4: Driving mechanism schema with nozzle and testing plate

3 Statistical methods

The data received from experiments were processed by several statistical techniques to determine the influence of surface roughness on heat transfer. The **Analysis of Variance (ANOVA)** was used to proof the influence. **One-way ANOVA** decomposes statistical population into several sets and is searching for significant differences of illustrated groups in *Fig.5*. This technique compares the means within selected groups as shown in the following model: $Y_{ij} = \mu + \alpha_i + \varepsilon_{ij}$, where Y_{ij} is for measured values, μ fixed but unknown constant, α_i group effect and ε_{ij} random noise with $N(0, \sigma^2)$ distribution. Index i represents a number of groups and j a number of measurement within each group. Current model can be also presented by this formula: $Y_{ij} = \mu_i + \varepsilon_{ij}$, where is $\mu_i = \mu + \alpha_i$. The ANOVA table decomposes the variance of population into two components: a between-group component and a within-group component and is testing whether there are any significant differences among the means. The F-test in the ANOVA table will test the null hypothesis that: $\alpha_i = 0$ for all $i=1, \dots, I$ or $\mu_1 = \mu_2 = \dots = \mu$. Alternative hypothesis is valid if at least one $\alpha_i \neq 0$ or $\mu_i \neq \mu$. Since the P-value of the F-test is less than 0,05, there is a statistically significant difference between the population mean from one level of chosen factor to another at the 95% confidence level. To determine which means are significantly different from the rest the **Scheffe**, **Duncan**, **LSD**, **Tukey**, **Bonferroni** a **Student-Newman-Keuls** tests were used (*Fig.6*). These tests are known as the Multiple Range Tests.

For ANOVA, a normal distribution is usually assumed for proceeding population as well as the independence among the groups. Several tests were run to determine whether population can be adequately modelled by a normal distribution. The **Chi-square Test** divides the range of population into non-overlapping intervals and compares the number of observations in each class to the expected number based on the fitted distribution. The **Kolmogorov-Smirnov Test** computes the maximum distance between the cumulative distribution of population and fitted normal distribution. The **Shapiro-Wilks Test** is based upon comparing the quantiles of the fitted normal distribution to the quantiles of the data. The **Standardized Skewness Test** looks for a lack of symmetry in the data. The **Standardized Kurtosis Test** looks for a distributional shape which is either flatter or more peaked than the normal distribution. Since the smallest testing P-value among the tests performed is greater than or equal to 0,05, we cannot reject the idea that current population comes from a normal distribution with 95% or a higher confidence. If the lowest P-value among the tests performed is less than 0,05, we can reject the idea that population comes from a normal distribution with 95% confidence.

The **Kruskal-Wallis Test** and **Variance Check** were used because not all proceeding population has required the distribution with sufficient confidence as well as outliers were detected in data. The Kruskal-Wallis Test, comparing the medians instead of means, tests the null hypothesis so that the medians of population within each level of the factor are the same. The data from all the levels is first combined and ranked from the smallest to largest ones. The average rank is then computed for the data of each level. Since the P-value is less than 0,05, there is a statistically significant difference among the medians at the 95,0% confidence level. To determine which medians are significantly different from the others, Box-and-Whisker Charts were plotted (Fig.7). In Variance Check four statistics test the null hypothesis of the standard deviations of population within each of the factor's levels are the same. As usual the 95,0% confidence level was considered. To verify the adequacy of ANOVA model the Residual Plots were applied (Fig.8). If the model suits for the current data the residual parameters in graph should have a normal distribution around 0-axis.

In contrast to one-way **Multifactor ANOVA** performs the analysis of variance for several different factors to determine which one has a statistically significant effect on population. It also tests for significant interactions among the factors as shown in the following model: $Y_{ijp} = \mu + \alpha_i + \beta_j + \gamma_{ij} + \varepsilon_{ijp}$, where Y_{ij} is for measured values, μ fixed but unknown constant, α_i 1st group effect, β_j 2nd group effect, γ_{ij} interaction effect and ε_{ij} random noise with $N(0, \sigma^2)$ distribution. The F-tests in the Multifactor ANOVA identify the significant factors and interactions. For each significant factor, the Multiple Range Tests determine which means are significantly different from the other. The Interaction Plot interprets (Fig.9) the significant interaction effects on population. The Residual Plots judge whether the assumptions of normal distribution in Multifactor ANOVA model suits to the real data.

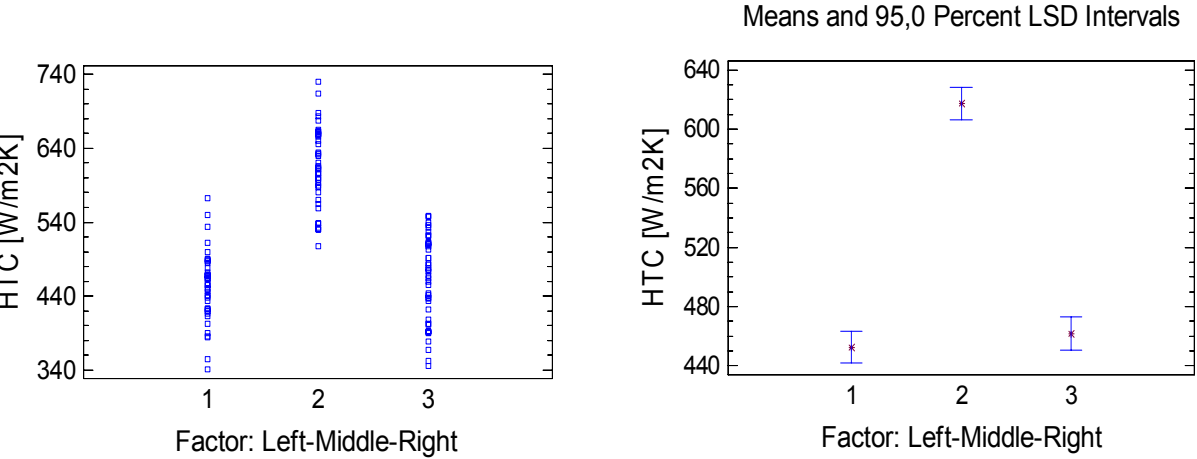


Fig. 5 (left) Dot Chart with decomposed data into 3-level factor (left-middle-right row from testing plate) shows significant difference between level 2 and 1, 3.

Fig. 6 (right) Decomposed data, mean and Scheffe's 95,0% confidence level

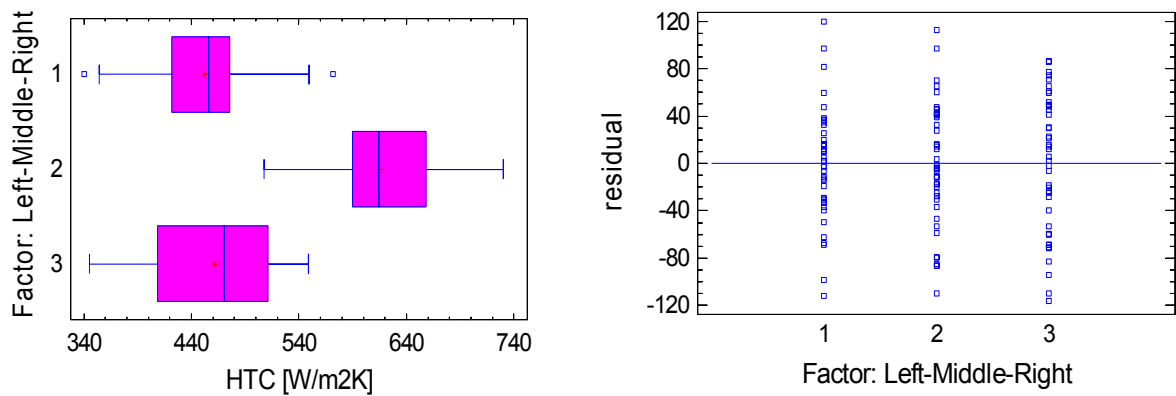


Fig. 7 (left) *Box-and-Whisker Plot for decomposed data (3-levels factor)*
Fig. 8 (right) *Residual Plot for decomposed data (3-levels factor) shows normal distribution for random noise*

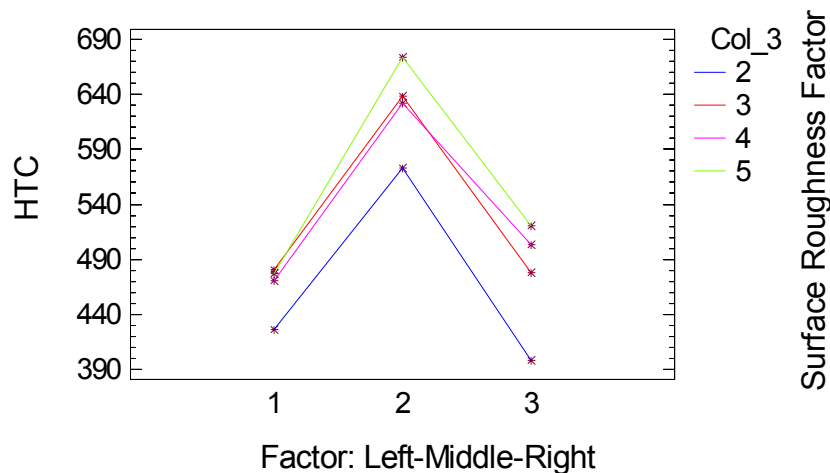


Fig. 9 *Interaction Plot compares influence between Surface Roughness and Position Factor*

4 Results and discussion

The methods mentioned above were applied to identify a supposed roughness influence on heat transfer. For our purposes the experimentally data received were subdivided into three independent sets with highly dissimilar characteristics. The first set is related to the temperatures and HTC above the Leidenfrost temperature (fig. 10 and 11). The second set describes physical aspects of cooling in the area close to Leidenfrost point surroundings. The third set shows the functionalities below the Leidenfrost point. Exact determination of roughness effects on heat transfer requires a precise identification of the Leidenfrost temperature. For purposes of ANOVA positions in rows (roughness factor) and columns (factor of position) these were chosen as determining factors. The second factor was chosen

for testing the accuracy of ANOVA methods, because the water impact distributions of the nozzles are known. Figures 5- 9 show a good agreement with Gaussian impact pressure distribution of flat nozzle in Fig. 12.

In the **high-temperature area** (above $T_{Leidenfrost}$) roughness was detected by ANOVA and by Kruskal-Wallis test as well as the significant factor with 99% confidence. The differences in average HTC between original (rolled) and manufactured surfaces are in a range of 10-18% increase in the nozzle axis and in a range of 9-22% increase of both plate edges (Figs. 13-15). The differences between manufactured surfaces, less than 6%, cannot be supposed as significant because the variances between repeated experiments have a similar order. However it must be mentioned that usually burnished surfaces have bigger HTC than fine grind surface and fine grind surface bigger than rough grind. Thus can be explained the results of material degradation exposed to high temperatures for a long time period.

In the **areas below Leidenfrost point** there are also statistically significant dependent on surface roughness (fig. 16), but with the confidence of 95% (in some cases even less). In two samples even differences were not found or results were dissimilar from others. In this area a rapid increase of transferred heat of original surface occurs, as well as an increase of burnish surface. Lower values for grind surfaces were observed. These, sometimes antagonistic, behaviours, are the results of major variances in the experiments within low-temperature phase.

Nearby Leidenfrost point the value of the Leidenfrost Temperature was used to determine surface roughness influence to heat transfer. Average HTC values couldn't give relevant results, because this area is quite short and sufficient data is not available. The experimental analysis shows the shifts of Leidenfrost point corresponding with the different surface of manufacturing methods (Fig. 17). Fig. 17 shows the increase of $L_{Leidenfrost}$ for original surface and decrease for burnish surface. It was also found, that values of $L_{Leidenfrost}$ are usually bigger in nozzle axis than in plate edges.

For more detailed surface recognition all usual roughness parameters were measured by mechanical and optical methods and recorded by electron microscope as well. A large amount of analyzed roughness parameters is necessary to identify the physical aspect of the differences of heat transfer discovered by statistical methods. The samples were treated before and after the experiment to identify a degree of surface roughness degradation. The Figures 18-20 illustrate the situation and show a typical rolled surface.

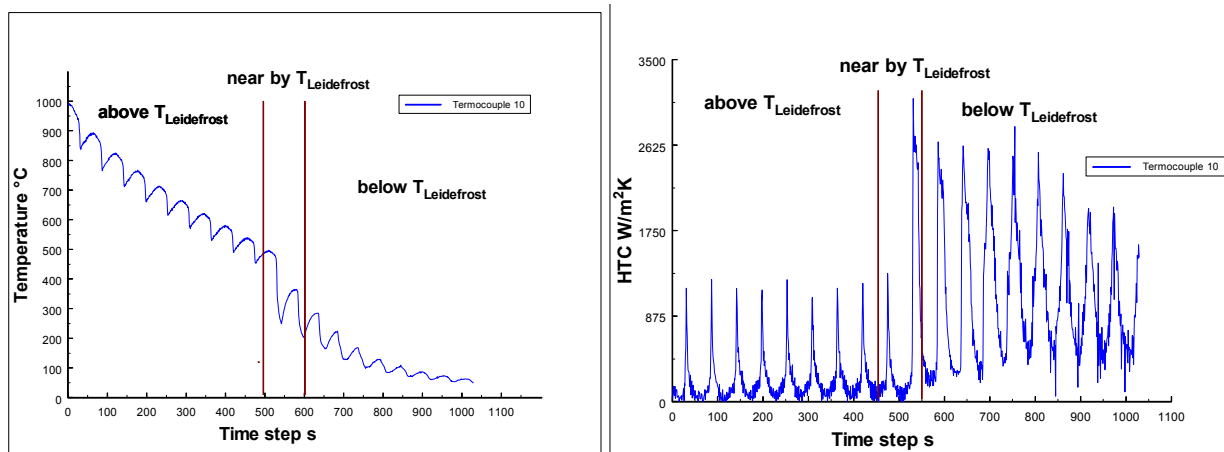


Fig. 10 (left) Temperature history with highlighted sets above, nearby and below $L_{Leidenfrost}$

Fig. 11 (right) HTC history with highlighted sets above, nearby and below $L_{Leidenfrost}$

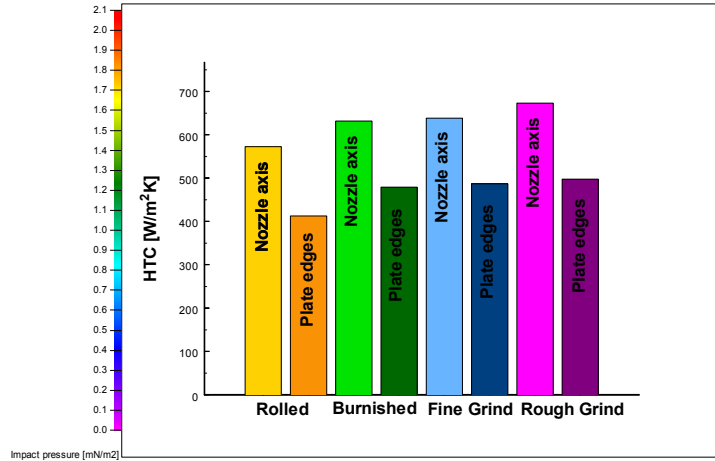
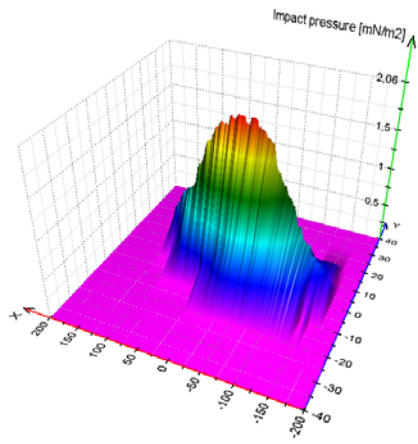


Fig. 12 (left) Water impact pressure distribution for flat nozzles

Fig. 13 (right) Average HTC for different surfaces and positions above Leidenfrost point

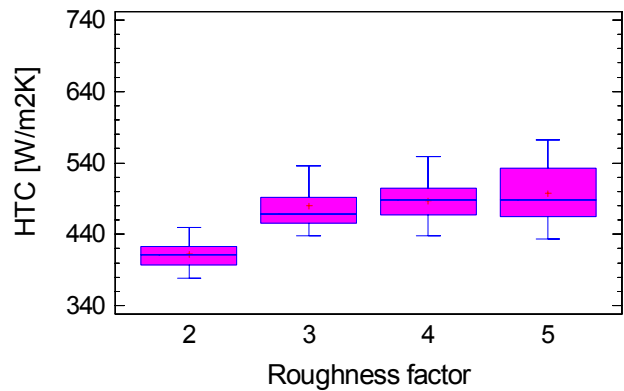
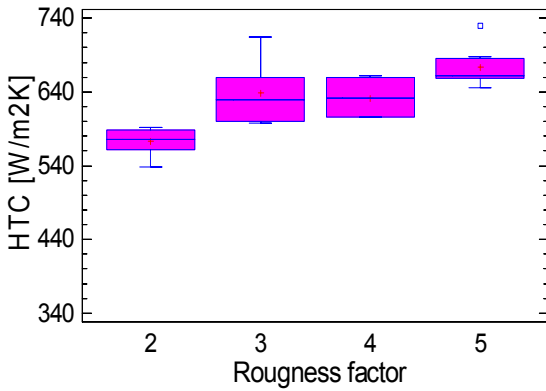


Fig. 14 (left) Box-and-Whisker Plot of HTC for roughness factor in nozzle axis

Fig. 15 (right) Box-and-Whisker Plot of HTC for roughness factor in plate edges

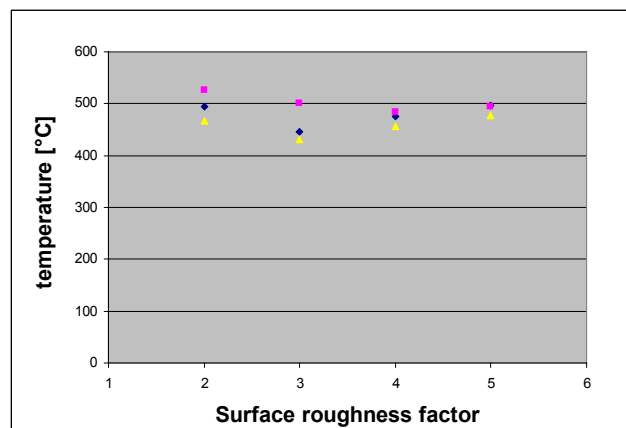
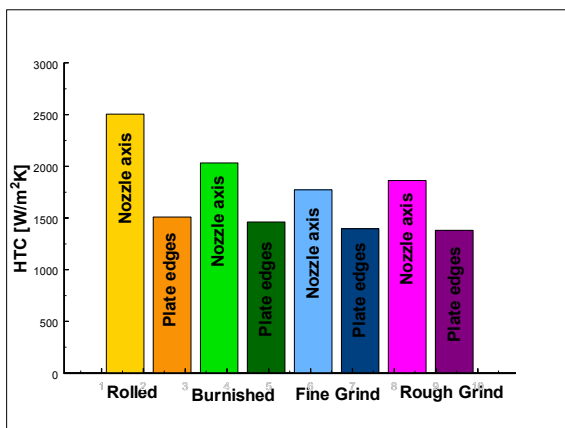


Fig. 16 (left) Average HTC for different surfaces and positions below Leidenfrost point

Fig. 17 (right) Leidenfrost temperature for all treated surfaces; original (rolled), burnished, fine and rough grind

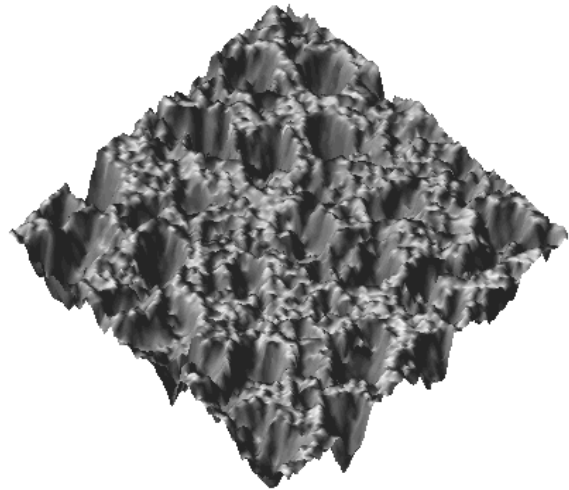
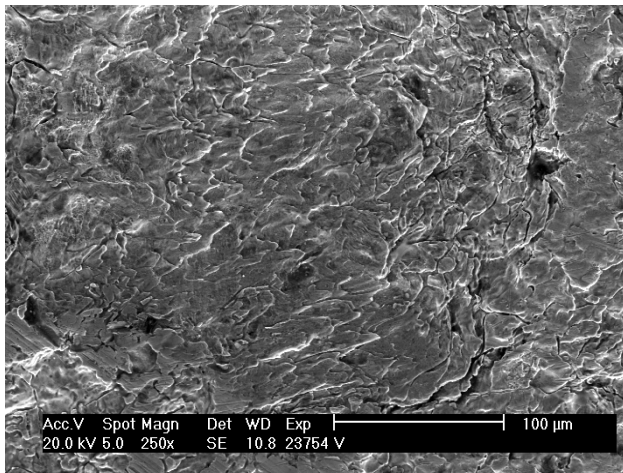


Fig. 18 (left) Photo of original rolled surface from electron microscope

Fig. 19 (right) 3D representation of original rolled surface

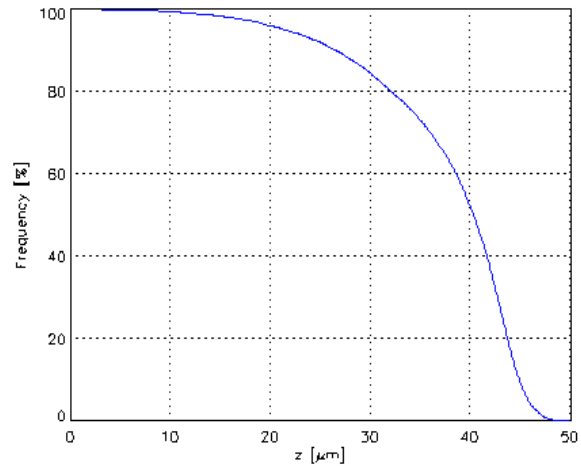
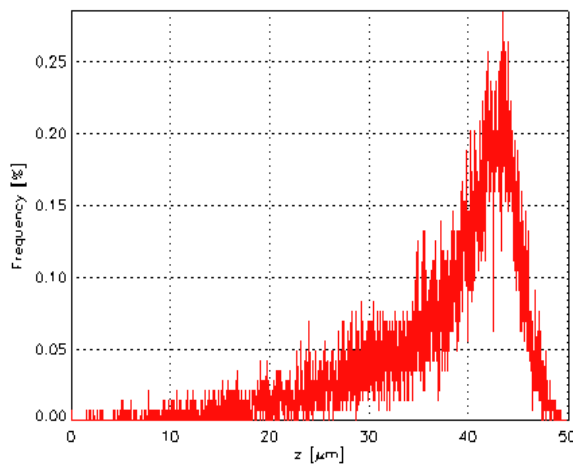


Fig. 20 Histogram (left) and distribution curve (right) for original rolled surface

5 Conclusion

The experiments with different surface roughness parameters were performed and various statistical methods applied to find out the influences on heat transfer in high-temperature ranges. The samples were tested by mechanical and optical roughness methods to identify which parameters have major effects. The key conclusions of the paper are as follows:

- 1) Statistical significant differences of heat transfer through surfaces manufactured in different way were found and the variances of Leidenfrost points were observed as well
- 2) Changes in surface roughness (in a range of 70-450% in Ra parameter) caused by thermal stress during experiments occur
- 3) In high-temperature area (above $T_{Leidenfrost}$) the differences in average HTC between original (412 W/m²K in plate edges, 572 W/m²K in nozzle axis) and manufactured surfaces (479-497 W/m²K in plate edges, 631-673 W/m²K in nozzle axis) were found

in a range of 10-18% increase in nozzle axis and in a range of 9-22% increase of both plate edges. The differences between manufactured surfaces are less than 6%.

- 4) In the areas below Leidenfrost point a rapid increase of transferred heat from original surface occurs (1510 W/m²K in plate edges, 2506 W/m²K in nozzle axis), as well as an increase of burnish surface (1460 W/m²K in plate edges, 2033 W/m²K in nozzle axis). Lower values for grind surfaces were observed (around 1390 W/m²K in plate edges, 1777-1862 W/m²K in nozzle axis).
- 5) Surface roughness influences cooling rate by creating microscopic (1-10µm) pits, which extend bubble formation. This effect can explain the increase of heat transfer for manufactured surfaces (burnished, fine and rough grind) with the roughness frequency mostly in a range of 0.5-6µm.
- 6) Surface roughness influences cooling rate by creating large (20-1000µm) roughness feature, which affect the Leidenfrost temperature. This effect can explain the increase of the Leidenfrost temperature and consecutively heat transfer for original rolled surfaces with the roughness frequency mostly around 45µm.

The results are in good agreement with our assumption and with the articles by Bernardin J.D. & Mudawar I., where similar conclusions were published.

REFERENCIES:

- Anděl J. (1993) Statistické metody, Matfyzpress
- Bernardin J.D. & Mudawar I. (2002) A Cavity Activation and Bubble Growth Model of the Leidenfrost Point
- Bernardin J.D. & Mudawar I. (1994) An Experimental Investigation into the Relationship between Temperature-history and Surface Roughness in the Spray Quenching of Aluminium Parts
- Bernardin J.D. & Mudawar I. (1995) Experimental and statistical investigation of changes in surface roughness associated with spray quenching
- Bernardin J.D. & Mudawar I. (1999) The Leidenfrost Point: Experimental study and assessment of existing models
- Bernardin J.D.; Stebbins C.J. & Mudawar I. (1996) Mapping of impact and heat Transfer Regimes of water drops impinging on a polished surface
- Horský J.; Raudenský M. & Šarler B.: Secondary cooling in continuous casting
<http://ucebnice.euromise.cz>, Základy statistiky – Analýza rozptylu
<http://www.uku.fi/~mauranen/advbis/advbis4.htm> - Analysis of variance and covariance
- Incopera, F. P. & De Witt D. P. (1990) Fundamentals of Heat and Mass Transfer, Third Edition
- Karpíšek Z. (2003) Statistika – lecture collection
- Köhler Ch.; Jeschar R.; Scholz R.; Slowik J. & Borchardt G. (1990) Influence of oxide scales on heat transfer in secondary cooling zones in the continuous casting process
- Raudenský M.; Horský J. & Kotrbáček P. (2004) The influence of surface roughness on the intensity of spay cooling in high temperature application, Technical report
- Raudenský M.; Horský J.; Kotrbáček P. & Kloss O. (2004) Heat transfer coefficient measurements for bloom continuous casting, Technical report